Low-energy-electron transmission in solid krypton and xenon films

I. T. Steinberger* and A. D. Bass†
Groupe du Conseil de Recherches Médicales en Sciences des Radiations, Faculty of Medicine, University of Sherbrooke, Sherbrooke, Quebec, Canada J1H5N4

R. Shechter
Racah Institute of Physics, The Hebrew University, Jerusalem 91904, Israel

L. Sanche
Groupe du Conseil de Recherches Médicales en Sciences des Radiations, Faculty of Medicine, University of Sherbrooke, Sherbrooke, Quebec, Canada J1H5N4

(Received 3 May 1993)

Low-energy-electron-transmission (LEET) spectra of krypton and xenon films deposited on a platinum substrate exhibit a peak at an energy somewhat below the center of the respective $\Gamma_{3/2}n=1$ exciton band. The peaks were systematically studied as a function of the film thickness. They were attributed to a process in which an electron loses a large part of its energy by creating a $\Gamma_{3/2}n=1$ exciton and consequently ends up in the conduction band of the rare-gas solid beneath the vacuum level. A simple model was formulated, taking into account the shape of the optical-absorption band and the image forces at the sample boundaries. Fitting the position, width, and height of the experimentally observed peaks in the thickest films (~ 100 monolayers or more) lead to the determination of the conduction-band energy V_0 and exciton band parameters in good agreement with the results of photoelectric and optical-absorption experiments. However, for thinner films the LEET peaks were much broader than predicted by theory. The possible reasons for this behavior are discussed in brief.

I. INTRODUCTION

During the past decade, many systematic studies were made concerning the evolution of electronic states characteristic of extended three-dimensional solids or liquids. In this respect, one of the central aims of the study of clusters has been to bridge the gap between atomic or molecular properties and those of the solid state. The evolution of various properties with cluster size has been investigated in many different substances.[1] Particularly relevant to the present work has been the study of clusters of rare gases, where the evolution of optical absorption and emission bands was described and analyzed in detail.[2–4] For the rare gases, evidence is also available on the evolution of several properties with the increase of the density from the dilute gas to the triple-point liquid and even the solid.[5,6] These properties include energies of high Rydberg states of a molecular impurity[7–9] (in the gas phase), the threshold of intrinsic[10] and impurity[11–13] photoconductivity, intermediate[14,15] and Mott-Wannier exciton energies[11,13] (in the liquid and the solid), electron and exciton effective masses[11,13] (in the liquid and the solid), electron mobilities,[16–18] and the energy V_0 of a thermalized conduction electron.[19,20]

This work deals with the evolution of bulk electronic properties of solid films of rare gases with layer thickness. Obviously this problem is relevant for other thin semiconductor or insulator layers as well, e.g., quantum wells. Rare-gas solids are of particular interest, since they are the simplest photoconductors. Moreover, ballistic electrons were studied in rare-gas solids (RGS's) in 1985: electron interference effects in thin films of solid argon and methane enabled direct determination of the dispersion (electron energy versus wave number) of the conduction band, including the energy V_0 of its minimum.[21]

The experiments described in this paper consisted of studying the transmission of low-energy (<15 eV) electrons through multilayer RGS films deposited on a Pt substrate. The transmitted currents were recorded as a function of the electron energy and the sample thickness. The structure observed in these low-energy-electron-transmission (LEET) spectra arises from two basic mechanisms.[22] (a) In the absence of inelastic scattering the transmitted current decreases rapidly with the increase of the sample thickness, since elastic scattering involves backscattering: electrons may return to the surrounding vacuum instead of arriving at the substrate.[23] (b) Inelastic scattering can cause an increase of the electron transmission, especially if the total energy of an electron *after* the loss by inelastic scattering lies below the vacuum level and above the energy V_0 of the bottom of the conduction band (measured with the vacuum level as a reference; we deal with cases where $V_0<0$).[24,25] If such an inelastic scattering event takes place, then the electron cannot be scattered back into the vacuum, since its energy is now below the vacuum level. On the other hand, it can be readily collected by the metal substrate.[24,25]

A pronounced rise was, indeed, observed[26] in the LEET spectra of thin films of krypton and xenon at the electron energy near to that of the $\Gamma_{3/2}n=1$ exciton. In the present work, this rise has been studied systematically as a function of the sample thickness. The results were

analyzed by means of a simple model, taking expressly into account the change of the electron energy due to the image force, and assuming that the energy loss is determined by the band shape of the exciton. For the thicker films a very good fit to the data could be obtained, using the exciton parameters from optical-absorption spectroscopy.[27–29] The fitting procedure also led to the determination of V_0 in both substances. For thinner films, however, an unexpected broadening of the exciton feature appeared. Comparison with optical[27–29] and high-resolution electron-energy-loss[30] (HREEL) data showed that this broadening is not due to changes in the exciton band. It is closely related to the electron transmission within the band gap as previously observed in thin films of several substances with $V_0 > 0$ (e.g., argon, nitrogen, and *n*-hexane[31]).

II. EXPERIMENT

The high-resolution electron-transmission spectrometer used has been described in detail in the past.[22,24] It is housed in an ion-pumped ultrahigh-vacuum system reaching a base pressure of the order of 10^{-8} Pa at the location of the experiments. The electron source was a trochoidal monochromator.[32] Monoenergetic electrons (resolution ~80 meV) were collected on a platinum ribbon serving as substrate for the xenon and krypton films. A thin ceramic platelet between the ribbon and a copper block ensured good thermal contact and electrical isolation. The temperature of the block could be varied be-

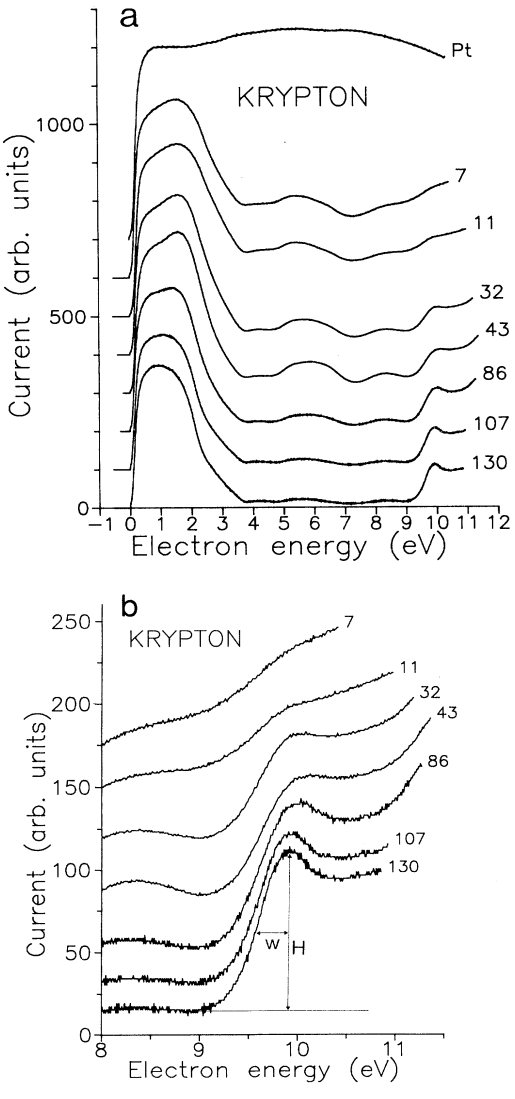

FIG. 1. Low-energy-electron-transmission (LEET) curves of krypton films. Vertically staggered. Pt-current without film, collected by the cleaned and annealed platinum ribbon substrate. The graphs are marked by the number of monolayers. (a) 0–11.3 eV. (b) Enlarged, 8–11.3 eV.

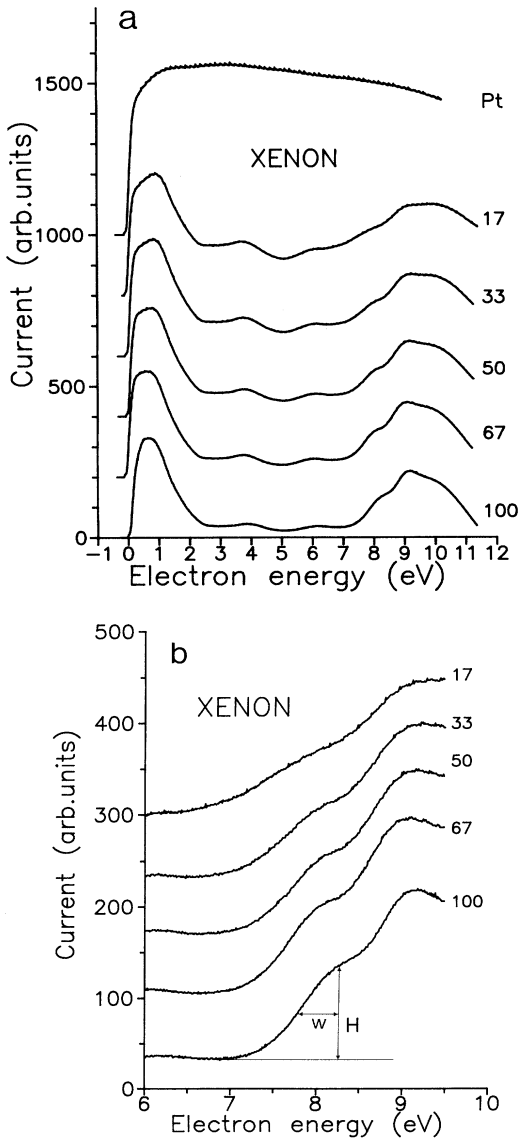

FIG. 2. LEET curves of xenon films. Vertically staggered. Pt-current without film, collected by the cleaned and annealed platinum ribbon substrate. The graphs are marked by the number of monolayers. (a) 0–11.3 eV. (b) Enlarged, 6–9.5 eV.

tween 15 and 300 K by means of a closed-cycle helium refrigerator. The currents measured were of the order of 10^{-9} A.

Before condensing the gases, the platinum ribbon underwent several cycles of heat treatment. A cycle consisted of heating in oxygen at a pressure of the order of 10^2 Pa to $\approx 1500\,^{\circ}$C for 10–20 s, followed by cooling to room temperature and heating again to an orange glow for about a minute. The effectiveness of the treatment was checked by recording (at room temperature) the current collected on the bare Pt substrate as a function of electron energy: the treatment was considered satisfactory, if the obtained curve was smooth with no local minima or maxima [see the uppermost curves of Figs. 1(a) and 2(a)]. The Pt ribbon surface cleaned in this manner had been previously characterized by the observation of low-energy-electron-diffraction (LEED) threshold interference structures.[33] The analysis indicated the presence of disordered Pt microcrystals with a large number of a microfacets having the (111) plane parallel to the surface with a strong azimuthal disorder. RGS's are expected to grow on Pt (111) crystallites according to the fcc (111) orientation with similar azimuthal disorder.[34] The films were grown from Matheson research grade gases without further purification. The solid krypton films were prepared by condensing the gas onto the cleaned and annealed Pt ribbon at ~ 17 K; to ensure better crystallinity the xenon films were deposited at around 30 K. The calibration of the sample thickness was made by means of the LEET spectrum itself: a thick layer of the rare gas was deposited and the LEET spectrum was recorded. Upon gradual heating this spectrum changed almost continuously with the temperature, as the RGS film evaporated, up to a point where the spectrum became stationary; at this temperature and beyond (until the next change in the spectrum) the transmission spectrum corresponds to that of 1 monolayer.[24] By trial and error we determined the dose of the rare gas necessary to obtain (at 17 K in Kr, 30 K in Xe) such a transmission spectrum: this dose served as a standard for calibration. With this procedure, the thickness of the sample was determined to an accuracy of about $\pm 10\%$, assuming layer-by-layer growth.

Eventual charging of the films manifested itself by a gradual washing out of various features in the LEET spectrum and by changing the energy of the initial sharp rise near zero energy. In films thinner than ~ 150 monolayers no charging was detected during an experiment.

III. RESULTS

Figure 1(a) shows a set of LEET spectra for krypton, as a function of the sample thickness, including the current versus electron energy of the cleaned and annealed platinum substrate. The excitonic feature of interest for this paper lies between 9 and 10 eV; an appropriate enlargement of the region above 8 eV appears in Fig. 1(b). A similar set of transmission curves for xenon is presented in Fig. 2(a); an enlargement appears in Fig. 2(b). There is a strong similarity between the curves of Figs. 1(a) and 2(a). In both sets there is a high, broad peak at the lowest

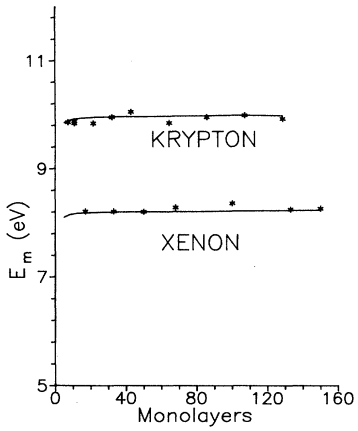

FIG. 3. The energy E_m of the maximum of the excitonic feature in krypton and xenon films, as a function of the number of monolayers K: asterisk, experiment; solid line, theory.

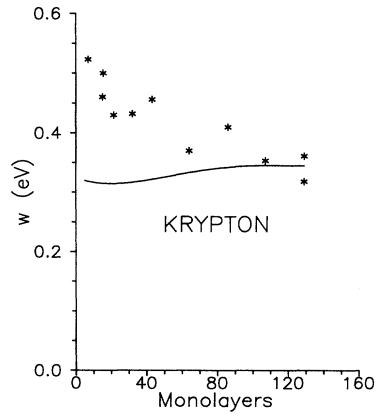

FIG. 4. The half-width w of the excitonic feature in krypton films, as a function of the number of monolayers K: asterisk, experiment; solid line, theory.

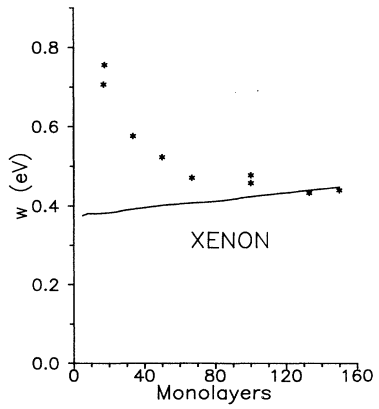

FIG. 5. The half-width w of the excitonic feature in xenon films, as a function of the number of monolayers K: asterisk, experiment; solid line, theory.

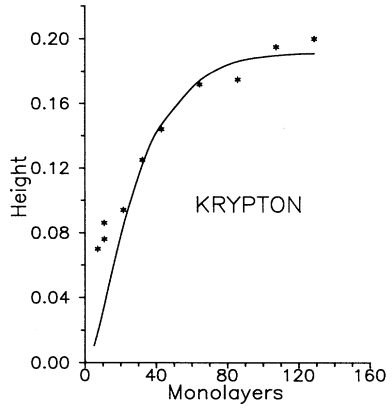

FIG. 6. The height H of the excitonic feature in krypton films, as a function of the number of monolayers K: asterisk, experiment; solid line, theory.

electron energies; at these energies the electrons move in the conduction band of the RGS, above the vacuum level. The small humps between the peak just above $E=0$ and between the features around 10 eV in Kr and 8 eV in Xe had been interpreted as being associated with the electronic band structure.[35] Returning to the excitonic features of Figs. 1(b) and 2(b), it can be seen that for the thinnest layers shown these are barely visible. In still thinner layers they could not be observed at all. On the other hand, the excitonic bands seem to be fully developed already in films of about 50 monolayers.

It should be noted that only the left-hand side of the peaks (up to the maximum or to the center of the shoulder) can be readily analyzed; this will be explained in the discussion section. In order to deal with the thickness dependence of the various features of the peaks, we defined the energy of the maximum E_m, its half-width at half maximum w, and its height H [see Figs 1(b) and 2(b)]. In cases where a shoulder was only observed, the value of E_m was determined from the local minimum of the first derivative of the LEET spectra. H was normalized to the current collected at the corresponding electron energy by the clean platinum surface.

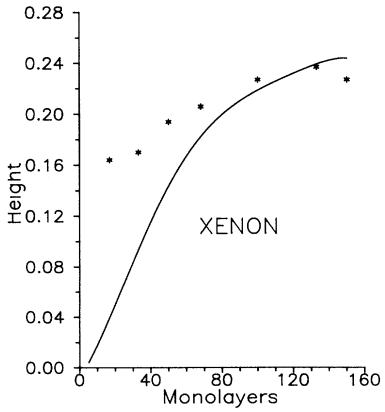

FIG. 7. The height H of the excitonic feature in xenon films, as a function of the number of monolayers K: asterisk, experiment; solid line, theory.

Figure 3 shows the value of E_m as a function of sample thickness for both krypton and xenon. Figures 4 and 5 represent the half-width w for krypton and xenon, respectively; Figs. 6 and 7 represent H. In these figures calculated curves also appear; see the discussion section below. Clearly, there is a good agreement between the experimental and calculated curves in Fig. 3. However, the calculated half-widths w agree with the experimental ones only for the thickest layers: the calculated peaks do not show the marked broadening observed in the experiments (Figs. 4 and 5). Moreover, the calculated heights H drop appreciably faster with decreasing thickness than the experimental ones (Figs. 6 and 7).

IV. THEORETICAL MODEL

The aim of our analysis was to formulate a model enabling a consistent discussion of the thickness dependence of the spectra, using, as far as possible, only data known from experiment. For this reason we did not employ the full probabilistic calculation of particle transport.[23] The actual model is a variant of the two-stream model;[25] it differs from the latter by using an integer variable instead of a continuous one, namely, the ordinal number of the monolayers instead of the distance from the sample surface. Moreover, the shape of the excitonic peaks, as observed in optical spectroscopy, is incorporated directly in the model. The simplifications of the two-stream model will be pointed out in the course of the following description of the model. Comparison with the two-stream model by Marsolais and Sanche[25] will be presented in the Appendix.

A. The recursion formulas

Consider a stream of electrons of energy E entering a sample extending from $z=0$ (sample-vacuum interface) to $z=L$ (sample-substrate interface); the sample consists of K monolayers of thickness a; in other words, $L=Ka$. For the moment we ignore inelastic scattering. Then, in any layer k of K monolayers the current density is the sum of two current densities: $J_0^+(k,E)$ flowing towards the substrate and $J_0^-(k,E)$ flowing in the opposite direction. $J_0^-(k,E)$ is generated by backscattering in layers with $k'>k$. Both $J_0^+(k,E)$ and $J_0^-(k,E)$ will refer to the plane between the $(k-1)$th and the kth layer. To simplify the notation, we will suppress from now on the energy dependence, except where it is essential for clarity. The current density $J_0(k)$ in the kth layer is

$$J_0(k)=J_0^+(k)+J_0^-(k) \tag{1}$$

with any k satisfying $1\le k\le K$, provided the sample does not become charged. In particular, assuming that electrons are not reflected at the metal substrate

$$J_0(K)=J_0^+(K)\ , \tag{2}$$

since under this assumption $J_0^-(K)=0$. Equation (2) is very useful as it enables the determination of the forward

current density in any layer of a sample.

The currents discussed until now are carried by hot electrons with energies well above the vacuum level. These have to be distinguished from the current carried by electrons that had suffered inelastic scattering and now have energies between the bottom of the conduction band and the vacuum level. Such an electron will be thermalized very quickly and fall to the bottom of the conduction band. After getting there it will have an extremely low probability of escaping back into the surrounding vacuum, since for such a process it would need an energy of the order of $|V_0| \sim 0.5$ eV (see below). Accordingly, we assume that every electron scattered inelastically remains in the sample and will eventually be collected by the substrate. This implies that all thermalized electrons arriving at the free surface of the sample will be reflected back into the sample.

It follows that if inelastic scattering also occurs, producing conduction-band electrons, this will cause: (i) a decrease of both the incoming and backscattered currents (J_0^+ and J_0^-) carried by the hot electrons and (ii) a generation of current J_1^+ flowing towards the substrate, carried by the conduction-band electrons. The incoming hot-electron current J_0^+ is now given by the recursion formula

$$J_0^+(k+1)=\left[J_0^+(k)+\frac{dJ_0^+(k)}{dk}\right][1-f(E)] . \tag{3}$$

The derivative refers to losses incurred by elastic backscattering and $f(E)$ is the fraction of hot electrons that are scattered inelastically into the conduction band below the vacuum level.

Because of the decrease in the concentration of hot electrons due to inelastic scattering, the current carried by the hot electrons alone cannot be determined from the dependence of the total current on K [Eq. (2)]. However, the *fraction* of hot electrons backscattered in any layer should be independent of the actual value of $J_0^+(k)$ and therefore

$$\frac{1}{J_0^+(k)}\frac{dJ_0^+(k)}{dk}=\frac{1}{J_0(k)}\frac{dJ_0(k)}{dk} . \tag{4}$$

By substitution into Eq. (3) we obtain

$$J_0^+(k+1)=J_0^+(k)\left[1+\frac{1}{J_0(k)}\frac{dJ_0(k)}{dk}\right][1-f(E)] . \tag{5}$$

The term containing the derivative can be determined by experiment from the thickness dependence of the total current at an electron energy where inelastic scattering is negligible.

The contribution to the current $J_1(k+1)$ in the $(k+1)$th layer by the conduction-band electrons (i.e., electrons that underwent inelastic scattering) is

$$J_1(k+1)=\left[J_0^+(k)+\frac{dJ_0^+}{dk}\right]f(E) . \tag{6}$$

By substitution and summing up the contributions of all K layers of the sample we get

$$J_1(K)=\sum_1^K J_0^+(k)\left[1+\frac{1}{J_0(k)}\frac{dJ_0(k)}{dk}\right]f(E) . \tag{7}$$

Equation (7) together with the recursion formula (5) enables the calculation of the total conduction-band current, provided $[dJ_0(k)/dk]/J_0(k)$ and $f(E)$ are known. Equations (5) and (7) do not violate the requirement of continuity of the current: this is ensured by the ingoing and backscattered hot-electron currents. In the above considerations we neglected the second-order process of inelastic scattering by previously backscattered electrons.

B. Calculation of the probability $f(E)$

The probability for an electron of energy E in the kth layer to be scattered inelastically and lose the energy η is nonzero, if the final state is an allowed one. As stated above, such an inelastically scattered electron will see a barrier at the sample surface and therefore will normally not escape into the surrounding vacuum. In other words, all inelastically scattered electrons will contribute to the LEET current if

$$V_0 < E-\eta < 0 . \tag{8}$$

The actual value of the probability df to lose energy between the $\eta+d\eta$ is considered to be dependent on the characteristics of the scatterer. We assume now that the scattering process is the creation of an exciton that can be approximately described as an absorption band of Gaussian shape and that df (at any given η) is proportional to the relative height of the band. In other words,

$$df=\frac{A}{\sqrt{2\pi}\alpha}\exp\left[-\frac{(\eta-E_1)^2}{2\alpha^2}\right]d\eta , \tag{9}$$

where E_1 is the position of the maximum of the band, α the width of the Gaussian, and A is a constant of proportionality related to the scattering cross section (see below). In view of condition (8), the total probability for inelastic scattering will be

$$f(E)=\frac{A}{\sqrt{2\pi}\alpha}\int_E^{E-V_0}\exp\left[-\frac{(\eta-E_1)^2}{2\alpha^2}\right]d\eta . \tag{10}$$

Actually an electron scattered into a conduction-band level just *above* the vacuum level should also have more chance to arrive at the substrate than an electron with high initial energy because of density-of-state and refraction effects.[25] In order to take this possibility into account in a very rough fashion we relaxed somewhat condition (8) writing

$$V_0 < E-\eta < \Delta E \geq 0 . \tag{8'}$$

ΔE is of the order of 0.1 eV. Accordingly, Eq. (10) becomes

$$f(E)=\frac{A}{\sqrt{2\pi}\alpha}\int_{E-\Delta E}^{E-V_0}\exp\left[-\frac{(\eta-E_1)^2}{2\alpha^2}\right]d\eta . \tag{10'}$$

E was determined by comparing the results of the calculations for the thickest layers with experiment.

If the electron moves in a layer far from both surfaces of the film, the energy E is equal to the energy E_0 of the incident electron, measured from the vacuum level. In the vicinity of the surfaces the correction W due to the image forces will be non-negligible:

$$E = E_0 - W \ , \tag{11}$$

where

$$W = -\frac{1}{2}\frac{e^2}{\epsilon a}\left[\frac{1}{2(K-k)} - \sum_{n=1}^{\infty}(M_{12})^n\left[\frac{1}{nK} - \frac{1}{2[(n-1)K+k]} - \frac{1}{2[(n+1)K-k]}\right]\right] , \tag{12}$$

with $M_{12}=(1-\epsilon)/(1+\epsilon)$, ϵ being the dielectric constant of the rare-gas solid, K the number of layers, k the index of the layer in question, and a the distance between adjacent close-packed layers (111). In the actual calculations the infinite sum was truncated at $n=10$. It should be noted that the energy pertaining to Eqs. (1)–(10) is also E, not E_0.

V. DISCUSSION

The experimental results were analyzed in the framework of the theoretical model described above, using Eqs. (5), (7), (10′), (11), and (12). The currents were normalized to the currents measured at the same electron energies, collected by the clean platinum electrode (without the sample). The layer number dependence of the current density $J_0(K,E_r)$ was determined at an electron energy E_r just below that of the excitonic feature. We found that the following relationship holds to a very good approximation:

$$J_0(K,E_r) = I_0 \exp(-a_1 K - a_2 K^2) \tag{13}$$

with $a_1 = 4.9\times10^{-2}$ and $a_2 = -2\times10^{-4}$ for Kr, while $a_1 = 2.7\times10^{-2}$, $a_2 = -6.58\times10^{-5}$ for Xe. Using Eq. (13) we substituted $(-a_1 - 2a_2 k)$ for the terms involving the derivative in Eqs. (5) and (7).

In order to compare the calculated and experimental excitonic features, sets of values were chosen (in a manner described below) for V_0, E_i, α, and E. With each set the expression

$$J_{\text{exc}}(K,E) \equiv J_0(K,E) + J_1(K,E) - J_0(K,E_r) \tag{14}$$

was calculated for fixed values of K and with E varying in the region of the excitonic peak. The values of J_{exc} thus obtained were then convoluted by a Gaussian in order to take into account the finite resolution of the system:

$$I_{\text{exc}}(K,E) = \frac{1}{\sqrt{2\pi}\sigma}\int_{-\infty}^{\infty}\exp\left[-\frac{\eta - E}{2\sigma^2}\right]J_{\text{exc}}(K,\eta)\,d\eta \ . \tag{15}$$

For both Kr and Xe we chose $\sigma = 0.1$ eV. In actual fact the limits of the numerical integration of (15) were taken from 8.8 to 11 eV for Kr and from 7.1 to 9.3 eV for Xe. Subsequently, the peak position E_m, half-width w, and height H of $I_{\text{exc}}(K,E)$ for a given K were determined and compared with the experimentally observed H, w, and E_m of the excitonic peak with the same K, referred to as E_r. E_m, w, and H appearing in Figs. 3–7 were obtained from such comparisons, after the parameters V_0, E_I, α, ΔE, and A (see below) were optimized.

The central consideration in the optimalization procedure was the requirement that the thickest films should behave like bulk solid krypton and xenon, i.e., our parameters should be in accord with the exciton parameters and with the values of V_0 determined by the best optical and photoelectric spectroscopic data. E_1 is determined to a very high accuracy by optical spectroscopy, so we chose our values of E_1 to agree with the best "optical" E_1.[27–29] V_0 is known less exactly[29,36,37] (especially for Kr) and thus we allowed deviation by up to 0.15 eV from photoelectric and spectroscopic data.[29,37] The width of the excitonic peak [represented by the Gaussian width α in Eqs. (9), (10), and (10′)] for solid krypton and xenon is known to be strongly dependent on the sample thickness and the quality of the crystallization;[27–29,37] therefore, we let it vary up to 0.16 eV. For comparison, we note that the smallest value of α is about 60 meV, reported for very thin films[27–29] ($\approx$30 nm). With these restrictions we tried to obtain a good agreement between experimental and calculated values of E_m and w for the thickest films. At first we put $\Delta E = 0$; this initial choice was satisfactory for Kr, but for Xe we had to choose $\Delta E = 0.18$ eV to obtain good agreement. The final values of the fitting parameters and their comparisons with optical and photoelectric results are summarized in Table I.

After optimizing the parameters E_1, w, α, and ΔE we found the dimensionless constant A directly from the height of the experimental peak in the thickest samples. A measures the inelastic scattering into the conduction band, to beneath the vacuum level [see Eq. (10)]. Since $|V_0|$ is considerably larger than α, there will be a range of values of E, at which the value of the factor multiplying A in Eq. (10) (including the integral) will be very near to unity. For such a value of E we have $A = n_0 S$, where n_0 is the number of atoms in one layer per unit area and S is the cross section for creating an exciton by inelastic scattering of hot electrons. For fcc (111) layers parallel to planes of the Pt(111) surface, we have[38] $n_0 = 7.18\times10^{14}$ cm^{-2} for Kr and $n_0 = 6.15\times10^{14}$ cm^{-2} for Xe. From here one obtains $S(\text{Kr}) \approx 10^{-16}$ cm^2 and $S(\text{Xe}) \approx 5\times10^{-17}$ cm^2. However, neglecting the reflections at the interfaces may appreciably affect the

TABLE I. Comparison of parameters obtained by fitting the theoretical model to experiments on the thickest films to parameters obtained by absorption spectroscopy and photoelectric experiments. E_1 is the energy of the first exciton peak ($\Gamma_{3/2}n=1$), α is Gaussian width. V_0 is the energy of the conduction electron with respect to the vacuum level and ΔE is the conduction-band correction (see text).

	Kr		Xe	
	This work	Literature	This work	Literature
E_1	10.17	10.173[a,b]	8.37	8.37[a]
α	0.16	0.06[b]	0.12	~0.08[a]
V_0	−0.44	−0.3[c]	−0.54	−0.59[d]
ΔE	0.0	· · ·	0.18	· · ·

[a]Reference 27. α is estimated for a film 2.7 nm thick.
[b]Reference 28. α is estimated for a film 3 nm thick.
[c]Reference 29.
[d]Reference 36.

values obtained for A and S.[23,26]

The fitting procedure dealt with only the values of E_m, w, and H, and not with the transmission curves directly. Even so, it can be seen (Figs. 8 and 9) that the fit to the transmission curves (in thick films) is also reasonable. We note in passing that we did not attempt to analyze the excitonic features beyond the maximum. The reason is that in this region a larger portion of the electrons are scattered into states within the conduction band that are just *above* the vacuum level. As we stated in connection with Eq. (10′), it is reasonable to assume that such electrons have fewer chances to get scattered back from the sample than the hot electrons with energies well above the vacuum level, because of density-of-states effects and refraction.[25] Since our quantitative knowledge about these electrons is practically nil, we did not analyze the curves beyond the "inelastic" maximum (or shoulder).

While the results of the calculations—using optical and photoelectric data—fit the present experimental results for the thick films well, there is a considerable discrepancy between the calculations and experiment for the thinner films. For such films the observed peaks are much broader and higher (especially for Xe) than the calculated ones. The broadening is towards lower electron energies. According to the model employed successfully for the thicker films, this should be attributed either to thickness-dependent changes of some parameter, or to processes feasible only in the thinner films. The various possibilities will now be discussed.

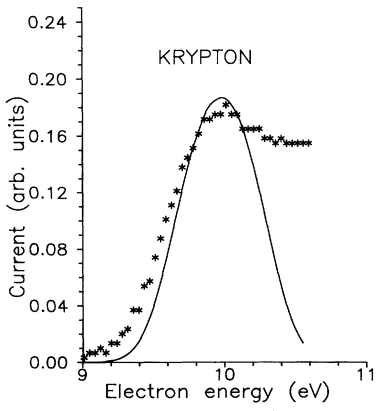

FIG. 8. Example for measured (asterisk) and calculated (solid line) current peak in a krypton film with $K=86$.

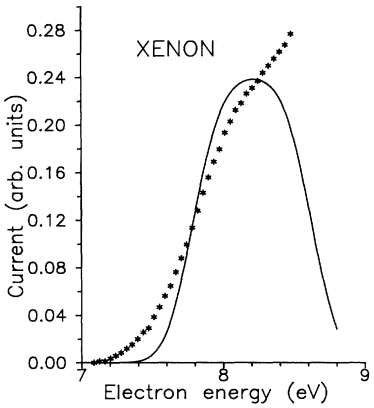

FIG. 9. Example for measured (asterisk) and calculated (solid line) current peak in a xenon film with $K=133$.

a. Excitons. A pronounced broadening of the exciton band in the thinner films would explain the effects observed. However, there is no theoretical basis to postulate such changes of the band shape. Moreover, the optical-absorption band corresponding to the exciton certainly does not broaden with decreasing layer thickness: on the contrary, it narrows slightly when the sample becomes thinner.[27,28] One should also note that the electron-exciton interaction in thin krypton and argon films has been studied recently by means of high-resolution electron-energy-loss spectroscopy (HREELS):[30] there is not indication in the experiments for any broadening of the excitonic band. It should be noted that for HREELS the conduction-band energy V_0 is irrelevant.

Both optical-absorption spectroscopy[27–29] and HREELS (Ref. 30) are able to resolve the $n=1$ surface exciton, at an energy 0.25–0.4 eV below that of the $n=1$ bulk exciton. In the LEET measurements presented here the surface exciton is not resolved. However, for $K=16$ the area under the surface exciton peak in, e.g., the HREELS measurements,[30] is less than 5% of the bulk exciton peak in solid Kr and less than 10% in solid argon. The ratio decreases further with increasing K. It follows that the observed broadening in LEET in the thinner films cannot be attributed to the unresolved contribution of surface excitons.

b. Conduction-band energy. To explain the observed effects, $|V_0|$ ought to increase considerably with decreasing thickness. There does not seem to be any theoretical or experimental justification to postulate such a behavior of V_0.

c. Other possibilities. According to the theoretical model presented, the low-energy tail of the excitonic feature would arise from electrons scattered inelastically

into the band gap and proceeding somehow within the forbidden gap to the platinum surface. Indeed, transmission of electrons of energy $E < V_0$ was observed[31] through thin layers of substances having a positive V_0 (argon, nitrogen, *n*-hexane). For argon, which seems to be the case nearest to the one presented in this paper, quantum tunneling was postulated, but the very long penetration lengths (up to 20 monolayers) present a serious difficulty.[31] Accordingly, it was suggested that states within the band gap (presumably associated with imperfect crystallization) assist the tunneling process.[31] The present case may be similar; however, we ought to assume now tunneling in even thicker films, up to about 50 monolayers. A major difficulty with this interpretation is the fact that even in liquid rare gases there is no evidence for any localized states below the bottom of the conduction band.[5,6]

Whatever the actual mechanism of the broadening of the excitonic feature, it seems that it is unavoidable to postulate a two-step process with a virtual intermediate state. Existence of band-gap states, as mentioned above, is one of several possibilities. One also might consider the interaction of the inelastically scattered electron with another entity as well, like a phonon in the rare-gas solid, or a surface plasmon in the metal substrate. As a result of the interaction *and* the inelastic scattering the electron would go directly to the bottom of the conduction band and from there to the metal. Even so it should be stressed that the present results (also taking into account the transmission of argon films at electron energies below the bottom of the conduction band) are insufficient to specify the actual mechanism responsible for the features observed in the thinner films.

ACKNOWLEDGMENTS

The authors wish to thank the Medical Research Council of Canada for making the experimental part of this work in Sherbrooke possible. Most calculations were made in Jerusalem with the support of the U.S.-Israel Binational Research Foundation, Grant No. 88-00107. I.T.S. is indebted to B. Laikhtman and L. Shvartsman for discussions.

APPENDIX

The relationship between the two-stream formulation of the hot- and thermalized-electron currents by Marsolais and Sanche[25] and the phenomenological model described this paper is presented below.

Equations (6) of Ref. 25 read as

$$\frac{dJ_0^+}{dz} = -(Q_{re}^0 + Q_i)J_0^+ + Q_{re}^0 J_0^- \ , \tag{A1}$$

$$-\frac{dJ_0^-}{dz} = -(Q_{re}^0 + Q_i)J_0^- + Q_{re}^0 J_0^+ \ , \tag{A2}$$

$$\frac{dJ_j^+}{dz} = -Q_{re}^j J_j^+ + Q_{re}^j J_j^- + (Q_{ri}^j + Q_{fi}^j)J_0^+ + Q_{ri}^j J_0^- \ , \tag{A3}$$

$$-\frac{dJ_j^-}{dz} = -Q_{re}^j J_j^- + Q_{re}^j J_j^+ + (Q_{ri}^j + Q_{fi}^j)J_0^- + Q_{ri}^j J_0^+ \ . \tag{A4}$$

Here the incoming and backstreaming hot-electron currents J_0^+ and J_0^- are regarded as a function of the distance z from the surface of the sample: in the notation of the present paper $z = ka$. J_j^+ and J_j^- are corresponding currents carried by electrons that underwent inelastic scattering into the jth inelastic channel. In the present case $j = 1$ and J_1^+, J_1^- denote currents thermalized to the bottom of the conduction band. The Q's are scattering probabilities: Q_{re}^0 refers to isotropic elastic scattering, Q_i to the total inelastic scattering, Q_{re}^j to elastic scattering of electrons that had been inelastically scattered previously, Q_{ri}^j to isotropic inelastic scattering of the hot electrons carrying the currents J_0^+ and J_0^-, and finally Q_{fi}^j to the forward inelastic scattering of the same.

In the paper we put $Q_{re}^j = 0$ and $Q_{ri}^j = 0$. Moreover, instead of Eqs. (A1) and (A2) we used the experimentally determined $J(k)$ at an electron energy where $Q_i = 0$ and we substituted subsequently for $-Q_{re}^0 J_0^+ + Q_{re}^0 J_0^-$ the expression $dJ_0^+(k)/dk$ in Eqs. (A1). With these changes the differential equations (A1) and (A3) become then the difference equations (3) and (6). In the present paper the shape of the optically observed exciton absorption band is employed to calculate the probability for inelastic scattering. The image forces both at the free surface and at the sample-substrate interface are taken into account. These points are not accounted for in Ref. 25.

---

*Permanent address: Racah Institute of Physics, The Hebrew University, Jerusalem 91904 Israel.

†Present address: Surface Analysis Research Centre, Dept. of Chemistry, UMIST, P.O. Box 88, Manchester M601QD, U.K.

[1]See, e.g., *Proceedings of the Fourth International Meeting on Small Particles and Inorganic Clusters, University Aix-Marseille III,* Aix-en-Provence, France, 5–9 July 1988, edited by C. Chapon, M. F. Gillet, and C. R. Henry [Z. Phys. D **12**, 1–4 (1989)].

[2]T. Möller and G. Zimmerer, J. Opt. Soc. Am. B **6**, 1062 (1989).

[3]B. Kamke, W. Kamke, Z. Wang, E. Ruhl, and B. Brutschy, J. Chem. Phys. **86**, 2525 (1987).

[4]T. Möller, Z. Phys. D **20**, 1 (1991).

[5]I. T. Steinberger, in *The Liquid State and its Electrical Properties,* edited by E. E. Kunhardt, L. G. Christophoru, and L. H. Luessen (Plenum, New York, 1988), p. 235.

[6]I. T. Steinberger, J. Chim. Phys. **90**, 681 (1993).

[7]A. M. Köhler, R. Reininger, V. Saile, and G. L. Findley, Phys. Rev. A **35**, 79 (1987).

[8]A. M. Köhler, V. Saile, R. Reininger, and G. L. Findley, Phys. Rev. Lett. **60**, 2727 (1988).

[9]I. T. Steinberger, U. Asaf, G. Ascarelli, R. Reininger, G. Reisfeld, and M. Reshotko, Phys. Rev. A **42**, 3135 (1990).
[10]R. Reininger, U. Asaf, I. T. Steinberger, V. Saile, and P. Laporte, Phys. Rev. B **28**, 3193 (1983).
[11]R. Reininger, S. Bernstorff, P. Laporte, V. Saile, and I. T. Steinberger, Chem. Phys. **86**, 189 (1984).
[12]R. Reininger, V. Saile, P. Laporte, and I. T. Steinberger, Chem. Phys. **89**, 473 (1984).
[13]M. Reshotko, U. Asaf, G. Ascarelli, R. Reininger, G. Reisfeld, and I. T. Steinberger, Phys. Rev. B **43**, 14 147 (1991).
[14]P. Laporte and I. T. Steinberger, Phys. Rev. A **15**, 2538 (1977).
[15]P. Laporte, J. L. Subtil, R. Reininger, V. Saile, S. Bernstorff, and I. T. Steinberger, Phys. Rev. B **35**, 6270 (1987).
[16]S. S. S. Huang and G. R. Freeman, J. Chem. Phys. **68**, 1355 (1978); Phys. Rev. A **24**, 714 (1981).
[17]F. M. Jacobsen, N. Gee, and G. R. Freeman, Phys. Rev. A **34**, 2329 (1986); J. Chem. Phys. **91**, 6943 (1989).
[18]G. Ascarelli, Phys. Rev. B **40**, 1871 (1989).
[19]R. Reininger, U. Asaf, and I. T. Steinberger, Chem. Phys. Lett. **90**, 287 (1982).
[20]R. Reininger, U. Asaf, I. T. Steinberger, and S. Basak, Phys. Rev. A **28**, 4426 (1983).
[21]G. Perluzzo, G. Bader, L. G. Caron, and L. Sanche, Phys. Rev. Lett. **55**, 545 (1985).
[22]L. Sanche, J. Chem. Phys. **71**, 4860 (1979).
[23]T. Goulet, E. Keszei, and J.-P. Jay-Gérin, Phys. Rev. A **37**, 2176 (1988); E. Keszei, T. Goulet, and J.-P. Jay-Gérin, *ibid.* **37**, 2183 (1988); **41**, 6006 (1990).
[24]R. M. Marsolais, M. Michaud, and L. Sanche, Phys. Rev. A **35**, 607 (1987).
[25]R. M. Marsolais and L. Sanche, Phys. Rev. B **38**, 11 118 (1988).
[26]G. Perluzzo, G. Bader, L.-G. Caron, and L. Sanche, Phys. Rev. B **26**, 3976 (1982); G. Bader, G. Perluzzo, L.-G. Caron, and L. Sanche, *ibid.* **26**, 6019 (1982).
[27]V. Saile, Ph.D. thesis, The University of Munich, 1976; quoted in *Electronic Excitations in Condensed Rare Gases* (Ref. 29).
[28]V. Saile, M. Skibowski, W. Steinmann, P. Gürtler, E.-E. Koch, and A. Kozevnikov, Phys. Rev. Lett. **37**, 305.
[29]N. Schwentner, E.-E. Koch, and J. Jortner, *Electronic Excitations in Condensed Rare Gases,* Springer Tracts in Modern Physics Vol. 107 (Springer-Verlag, Berlin, 1985).
[30]M. Michaud and L. Sanche (unpublished).
[31]L. G. Caron, G. Perluzzo, G. Bader, and L. Sanche, Phys. Rev. B **33**, 3027 (1986).
[32]P. Cloutier and L. Sanche, Rev. Sci. Instrum. **60**, 1054 (1989).
[33]M. Michaud, L. Sanche, C. Gaubert, and R. Baudoing, Surf. Sci. **205**, 447 (1988).
[34]J. A. Venables, J. L. Seguin, V. Suzanne, and M. Bienfait, Surf. Sci. **145**, 345 (1984).
[35]G. Bader, G. Perluzzo, L. G. Caron, and L. Sanche, Phys. Rev. B **30**, 78 (1984).
[36]I. T. Steinberger, I. H. Munro, E. Pantos, and U. Asaf, in *Vacuum Ultraviolet Radiation Physics,* edited by E.-E. Koch, R. Haensel, and C. Kunz (Pergamon-Vieweg, Braunschweig, 1974), p. 347.
[37]B. Sonntag, in *Rare Gas Solids,* edited by M. L. Klein and J. A. Venables (Academic, New York, 1977), Vol. II, p. 1021
[38]C. Kittel, *Introduction to Solid State Physics* 6th. ed. (Wiley, New York, 1986).